Burdon KP, Macgregor S, Hewitt AW, Sharma S, Chidlow G, Mills RA, Danoy P, Casson R, Viswanathan AC, Liu JZ, Landers J, Henders AK, Wood J, Souzeau E, Crawford A, Leo P, Wang JJ, Rochtchina E, Nyholt DR, Martin NG, Montgomery GW, Mitchell P, Brown MA, Mackey DA, Craig JE. (2011) Genome-wide association study identifies susceptibility loci for open angle glaucoma at TMCO1 and CDKN2B-AS1. Nature Genetics. 43(6): 574-8

DOI: http://dx.doi.org/10.1038/ng.824

Genome-wide association study identifies susceptibility loci for open angle glaucoma at *TMCO1* and *CDKN2B-AS1*

Kathryn P. Burdon[1]*, Stuart Macgregor[2]*, Alex W. Hewitt[1,3]*, Shiwani Sharma[1], Glyn Chidlow[4], Richard A. Mills[1], Patrick Danoy[5], Robert Casson[4], Ananth C. Viswanathan[6], Jimmy Z. Liu[2], John Landers[1], Anjali K. Henders[2], John Wood[4], Emmanuelle Souzeau[1], April Crawford[1], Paul Leo[5], Jie Jin Wang[3,7], Elena Rochtchina[7], Dale R. Nyholt[2], Nicholas G. Martin[2], Grant W. Montgomery[2], Paul Mitchell[7], Matthew A. Brown[5], David A. Mackey[3,8,9], Jamie E. Craig[1]

1 Department of Ophthalmology, Flinders University, Flinders Medical Centre, Adelaide, Australia.

2 Genetics and Population Health, Queensland Institute of Medical Research, Brisbane, Australia.

3 Centre for Eye Research Australia, University of Melbourne, Royal Victorian Eye and Ear Hospital, Melbourne, Australia.

4 South Australian Institute of Ophthalmology, Hanson Institute & Adelaide University.

5 The University of Queensland Diamantina Institute, Princess Alexandra Hospital, Brisbane, Australia.

6 Moorfields Eye Hospital, London, United Kingdom.

7 Centre for Vision Research, Department of Ophthalmology and Westmead Millennium Institute, University of Sydney, Westmead, Australia.

8 Lions Eye Institute, University of Western Australia, Centre for Ophthalmology and Visual Science, Perth, Australia.

9 Discipline of Medicine, University of Tasmania, Hobart, Australia.

*these authors contributed equally

Address for Correspondence:
Associate Professor Jamie Craig
Department of Ophthalmology
Flinders University
Flinders Drive
Bedford Park
South Australia, 5042

Telephone: (08) 8204 4899
Fax: (08) 8277 0899
Email: jamie.craig@flinders.edu.au

A genome-wide association study (GWAS) for open angle glaucoma (OAG) blindness was conducted using a discovery cohort of 590 cases with severe visual field loss and 3956 controls. Genome-wide significant associations were identified at *TMCO1* (rs4656461 (G) OR=1.68, $p=6.1x10^{-10}$) and *CDKN2B-AS1* (rs4977756 (A) OR = 1.50, $p=4.7x10^{-9}$). These findings were replicated in a second cohort of advanced OAG cases (rs4656461 p=0.010; rs4977756 p=0.042) and two further cohorts of less severe OAG. The study wide odds ratios are 1.51 (1.35-1.68), $p=6.00x10^{-14}$ at *TMCO1,* and 1.39 (1.28-1.51), $p=1.35x10^{-14}$ at *CDKN2B-AS1* (also known as *CDKN2BAS* and *ANRIL)*. Carriers of 1 or more risk alleles at both loci concurrently are at >3-fold increased risk of glaucoma. We demonstrate retinal expression of genes at both loci, and show that *CDKN2A* and *CDKN2B* are strongly upregulated in an animal model of glaucoma.

Glaucoma is a group of neurodegenerative ocular diseases united by a clinically characteristic optic neuropathy. It is the second leading cause of blindness worldwide[1]. Primary open angle glaucoma (OAG) is the commonest subtype[1]. OAG pathogenesis and factors determining disease progression are poorly understood. Early intervention with measures to reduce intraocular pressure retards visual loss in most individuals[2], but many cases of glaucoma remain undiagnosed until irreversible vision loss has occurred. Elucidation of SNPs associated with severe outcomes could enable better targeting of treatments which carry cost and morbidity, to individuals at highest risk of blindness. Linkage and candidate gene studies have identified several genes likely to be involved in OAG including myocilin[3] and *NTF4*[4], although for the latter, findings have varied in different populations[5]. A recent GWAS using Icelandic OAG cases of unselected severity identified association with variants near *CAV1*[6]. To identify genes predisposing individuals to OAG blindness, we performed a GWAS in Australian Caucasians with advanced OAG (individuals with OAG who have progressed to severe visual field loss or blindness).

Advanced OAG cases (N=590 after data cleaning) were selected from the Australian & New Zealand Registry of Advanced Glaucoma (ANZRAG) and the Glaucoma Inheritance Study in Tasmania (GIST)[7,8]. Two previously described Australian samples were used as controls (N=1801 and 2155, total 3956)[9]. Cohort demographics are given in Table 1 and recruitment and disease definitions are in the Supplementary Material. Samples were typed on Illumina arrays (Cases: Omni1; Controls: HumanHap610 or HumanHap660). Cases and controls were combined into a single data set for cleaning and imputation. All participants were Australian Caucasians of European descent.

After cleaning, 298,778 SNPs were available for association testing. The genomic inflation factor (λ) in the discovery cohort was 1.06 (Q-Q plots uncorrected and corrected for λ are in Supplementary Fig. 1A and B). The λ reduced to 1.04 when the first 10 principal components were included as covariates. The association results across the genome are displayed in Figure 1; results are presented corrected for $\lambda=1.06$, without correction for principal components. Results with correction for principal components were similar (data not shown). Two regions clearly reached genome-wide significance (defined at $p<5x10^{-8}$, Table 2), with $p=6.1x10^{-10}$ at rs4656461 (G) near the *TMCO1* gene on chromosome 1q24, and $p=4.7x10^{-9}$ at rs4977756 (A) in the *CDKN2B-AS1* gene on chromosome 9p21. Association results at these loci for both genotyped and imputed SNPs are shown in Figure 2. Imputation of SNPs from the 1000 Genomes project did not reveal any SNPs with substantially stronger association than the top genotyped SNPs (Fig. 2), or identify additional genome-wide significant loci. At both loci, the most associated SNP is supported by concordant results for other SNPs in moderate or high linkage disequilibrium.

Three replication cohorts were drawn from the Australian Caucasian population and are all of European descent (Table 1). The advanced glaucoma replication cohort consisted of 334 additional advanced OAG cases with 434 elderly controls. The less severe cohort consisted of 465 OAG cases and 1436 controls from the Wellcome Trust Case-Control Cohort 1958 Birth Cohort (WTCCC 58BC). The third cohort was a population based study, the Blue Mountains Eye Study, containing 93 cases of glaucoma and 2712 examined elderly controls. The most associated SNPs at each locus clearly replicated in all cohorts (Table 2). Other SNPs in both of these regions were also associated in the replication cohorts (Supplementary Table 1A). Combining all replication cohorts gave an odds ratio (OR) of 1.39 (95% CI, 1.20-1.61), $p=7.56x10^{-6}$ for rs4656461 near the *TMCO1* gene and 1.33 (1.19-1.48), $p=4.19x10^{-7}$ at rs4977756 in the *CDKN2B-AS1* gene (Supplementary Table 1B). All SNPs of interest are also still significantly associated following adjustments for age and sex in a logistic regression, indicating that the observed associations are independent of these parameters, despite the differences between case and control cohorts. We combined all available controls to enable a comparison of odds ratios for the risk alleles at both loci between the advanced OAG cohorts and the less severe OAG cases (Supplementary Table 1C). Stronger ORs were observed in the advanced cases, and these results support the hypothesis that the risk alleles identified are associated with all OAG, but are more strongly associated with cases which progress to advanced disease. Alternatively, higher diagnostic certainty in severe disease could account for this observation.

Combined analysis of discovery and all replication cohorts generated an overall OR 1.51 (1.35-1.68), $p=6.0x10^{-14}$ for rs4656461, and 1.39 (1.28-1.51), $p=1.35x10^{-14}$ for rs4977756. Haplotype analyses indicate three common haplotypes around *TMCO1* and two at *CDKN2B-AS1*. The overall p-value for association is $6.56x10^{-12}$ around the *TMCO1* gene and $2.59x10^{-9}$ at the *CDKN2B-AS1* locus (Supplementary Table 2). In both cases the risk alleles detected in the single SNP analysis are present on a single common haplotype which shows significant association. The haplotype with the alternative allele at each location appears to be protective against OAG development. Twelve OAG patients homozygous for the risk allele at rs4656461 were sequenced at all coding exons of the gene and the 3'UTR. Several common SNPs in the 3'UTR were found to be present on the risk haplotype although the functionality of these SNPs is not known (Supplementary Table 3). The lack of identified coding variants suggests the true causative variants are likely to be located in a regulatory region of *TMCO1*.

To obtain an unbiased estimate of risk for advanced glaucoma, we focused on the first replication cohort[10]. Taking these advanced glaucoma cases (N=334), the matched examined elderly controls (N=434), and similar age-matched controls from the BMES cohort (N=502), we fitted rs4977756 and rs4656461 in a logistic regression. Assuming an additive model, individuals carrying four risk alleles (two at each locus) had 4.50 (95% CI=1.84-11.01) fold higher risk of advanced OAG relative to non-carriers. Grouping individuals with one or two risk alleles together at both loci (dominant model), gave a 3.03 (95% CI=1.52-6.07) fold increased risk. Eighteen percent of the normal population are in this risk category.

Two control cohorts were used in this study; one a population sample based on parents of twins and the other a sample of endometriosis cases. Cases and controls were subjected to the same cleaning regime to ensure a well matched dataset. The male:female ratio was similar between the case cohort and the twin-based controls, but the endometriosis 'controls' were all female. We repeated the analysis excluding the endometriosis controls. The p-values at rs4656461 and rs4977756 changed to $p=5.3x10^{-9}$ and $p=1.1x10^{-7}$, respectively, with the reduced significance due to smaller sample size as allele frequencies are very similar between control cohorts (Supplementary Table 4A). X chromosome results were also similar. In addition, we utilised the Wellcome Trust Case-Control Cohort 1958 Birth Cohort (WTCCC 58BC) data as an alternative control cohort. Both loci reached genome-wide significance in this analysis, indicating that our findings do not represent an artefact of the historic controls utilised (Supplementary Table 4B, Supplementary Fig. 1C).

SNP rs4656461 at the 1q24 locus is ~6.5 kb downstream of the *TMCO1* gene. SNP rs4977756 at the

9p21 locus is located within the antisense RNA gene *CDKN2B-AS1*. This region also harbors the tumour suppressor genes *CDKN2A* and *CDKN2B* and is adjacent to the *MTAP* gene. *CDKN2A* also encodes an alternate open reading frame, *ARF*. We analysed expression of these genes in human ocular tissues by RT-PCR. All the genes are expressed in the iris, ciliary body, retina and optic nerve, but the expression levels varied among the analysed tissues (Fig. 3A). Furthermore, we determined which of the *CDKN2B-AS1* splice variants were expressed in the retina, the tissue ultimately compromised in glaucoma. RT-PCR revealed expression of three splice variants of this gene in the human retina (Fig. 3B). This is consistent with expression of more than one *CDKN2B-AS1* splice variants in a tissue or cell line[11,12]. We utilized well characterized antibodies directed against CDKN2A, CDKN2B, MTAP and TMCO1 to explore the distribution of these proteins in rat retina. CDKN2A and CDKN2B were expressed in retinal ganglion cells (RGC) and other retinal cell types displaying nuclear patterns of localization, similar to those reported in other tissues (Supplementary Fig. 2). TMCO1 was also associated with all retinal cells, but strongest expression was observed in RGC. MTAP was expressed at low levels in retinal astrocytes (data not shown). To ascertain whether these genes are candidates for involvement in the pathogenesis of glaucoma, we performed real-time PCR analysis of their expression levels in a validated rat model of glaucoma [13] (Fig. 4). Strong upregulation of expression of *Cdkn2a* and *Cdkn2b*, but not *Tmco1* was observed in the retina one week after induction of ocular hypertension, a time-point corresponding to ongoing RGC death, as indicated by axonal cytoskeleton damage in the optic nerve of the animals studied.

Recessive mutations in *TMCO1* cause a syndrome consisting of craniofacial dysmorphism, skeletal anomalies and mental retardation[14]. The gene encodes a transmembrane protein with a coiled-coil domain that may localise to the Golgi apparatus and endoplasmic reticulum[15] or to the mitochondria[16] in different cell types. In humans, the gene is ubiquitously expressed in developing and adult tissues[14]. The protein sequence is completely conserved among many mammalian species[14]. Although requiring experimental confirmation, Zhang et al proposed a role for TMCO1 in apoptosis[16]. This may suggest a mechanism for the association with glaucoma, which is characterised by excessive RGC apoptosis. It is also possible that other genes adjacent to *TMCO1* such as *ALDH9A1* could be responsible for the glaucoma association observed in this study.

CDKN2B-AS1 resides in the 9p21 region that has been clearly associated with cardiovascular disease [17], diabetes[18], intracranial aneurysm[19] and glioma[20]. The antisense RNA encoded by *CDKN2B-AS1* regulates neighbouring genes at 9p21, particularly *CDKN2B* with which its expression levels are reciprocally related[21]. CDKN2B and CDKN2A activate the retinoblastoma tumour suppressor pathway, whereas ARF activates the p53 tumour suppressor pathway. The 9p21 locus is activated in response to oncogenic stimuli[22]. The *CAV1* gene, recently reported to be associated with OAG[6], regulates mitogenic signalling and acts synergistically with *CDKN2A*[23]. Although the *CAV1* SNP (rs4236601) did not reach statistical significance in this GWAS ($p=0.17$ for a 1 sided test), the observed odds ratio of 1.07 is consistent with that previously reported in larger European cohorts, as are the allele frequencies (cases; 0.290, controls; 0.276 for A allele). It should be noted that many of the cases in the current study are included in the previously reported Australian replication cohort[6]. Genes at the 9p21 locus are known to play a role in aberrant cell division, and we propose that the 9p21 OAG risk variants may predispose RGCs to gradual apoptosis. This hypothesis is supported by observations that the opposite risk alleles in *CDKN2B-AS1* are associated with glaucoma and glioma. For example, at rs4977756 and rs1063192, the G and C alleles respectively, are protective for glaucoma but are the risk alleles for glioma[20]. The direction of association is the same for glaucoma as for cardiovascular disease[17] and diabetes[18], but further work is required to determine whether the same causative variant/s underlie these different disease associations.

Recently, rs1063192 in *CDKN2B* was reported to be associated at genome-wide significance with optic cup-to-disc ratio in normal individuals[24]. Nominal association of this SNP with glaucoma in a small case series was also reported[24]. In our study, this particular SNP had a p-value of 3.9×10^{-7} in the discovery cohort and the nearby SNPs in *CDKN2B-AS1* reached genome-wide significance. Thus, we provide further compelling evidence that the 9p21 region is a strong genetic risk factor for OAG in support of the previous suggestive association with OAG at this locus.

This study shows clear evidence of association of two genes, *TMCO1* and *CDKN2B-AS1* with advanced OAG, imparting a 3 fold increase in risk for carriers of one or more risk alleles at the two loci. In addition, we have shown strong upregulation of *CDKN2A* and *CDKN2B* in response to elevated intraocular pressure, further indicating that this region is important in the molecular pathways leading to glaucoma development. This discovery was made utilising a novel approach of selecting cases with severe blinding OAG for the GWAS, but as expected the risk alleles are also associated with less severe cases, demonstrating the efficacy of using extreme cases to identify genes for a common disease. OAG can be difficult to diagnose in the early stages, and these findings may be useful in the future to prioritise treatment effectively for glaucoma suspects in whom it is often difficult to decide upon timing of treatment initiation. As treatment for glaucoma is proven to slow disease progression[2], timely initiation of conventional treatment in those at highest risk could reduce glaucoma blindness. In addition, we have begun to elucidate novel biochemical pathways involved in this disease, which could lead to more targeted OAG treatment regimes aiming to protect RGC in ways other than lowering intraocular pressure which has hitherto formed the cornerstone of treatment.

WEB RESOURCES

EIGENSOFT: http://genepath.med.harvard.edu/~reich/Software.htm
MACH2: http://www.sph.umich.edu/csg/abecasis/MACH/index.html
1000 Genomes: http://www.1000genomes.org
PLINK: http://pngu.mgh.harvard.edu/~purcell/plink/
LocusZoom: http://csg.sph.umich.edu/locuszoom/
Australian & New Zealand Registry of Advanced Glaucoma: www.anzrag.com
European Genome-phenome Archive: http://www.ebi.ac.uk/ega/page.php

ACKNOWLEDGEMENTS

This research was funded by the National Health and Medical Research Council (NHMRC) of Australia, project grant 535074 to J.E. Craig et al. We also thank the following organisations for their financial support: RANZCO Eye Foundation, Clifford Craig Medical Research Trust, Ophthalmic Research Institute of Australia (ORIA), Pfizer Australia, Glaucoma Australia, American Health Assistance Foundation (AHAF), Peggy and Leslie Cranbourne Foundation, Jack Brockhoff Foundation, NEI Project Grant (2007-2010). The Australian Twin Registry is supported by an NHMRC Enabling Grant (2004-2009). The QIMR Study was also supported by grants from the NHMRC (241944, 339462, 389927,389875, 389891, 389892, 389938, 443036, 442915, 442981, 496610, 496739, 552485, and 552498), the Cooperative Research Centre for Discovery of Genes for Common Human Diseases, Cerylid Biosciences (Melbourne), and donations from Neville and Shirley Hawkins.

SM and KPB are supported by NHMRC Career Development Awards (496674, 613705, and 595944). DRN was supported by the NHMRC Fellowship (339462 and 613674) and ARC Future Fellowship (FT0991022) schemes. GWM, MAB and JEC are supported by the NHMRC

Fellowships Scheme. DAM is a recipient of the Pfizer Australia Senior Research Fellowship.

We thank all participants of ANZRAG, GIST, BMES, QIMR, OXEGENE, NHS and BATS studies and the staff who have collated clinical data and DNA samples over many years. We thank Glaucoma Australia and Endometriosis Associations for supporting study recruitment. We thank S. Nicolaides, Queensland Medical Laboratory and SA Pathology for pro bono collection and delivery of blood samples and other pathology services for assistance with blood collection.

We thank B. Usher, S. Thorpe, A. Kuot, A. McMellon, M. Ring, T. Straga, L. Kearns, J. Barbour, S. Staffieri, J.Ruddle, P.Coleman, M.J. Wright, M.J. Campbell, A.Caracella, L. Bowdler, S. Smith, S. Gordon, K. Zondervan, S. Treloar, J. Painter, B. Haddon, D. Smyth, H. Beeby, O. Zheng, and B. Chapman for their input into project management, databases, sample and data collection, sample processing and genotyping. We are grateful to the many research assistants and interviewers for assistance with the studies contributing to the collections used in this project.

We gratefully acknowledge the use of the Wellcome Trust Case Control Consortium 1958 British Birth Cohort data.

AUTHOR CONTRIBUTIONS:

KPB, SM, AWH, DAM, and JEC were involved in the concept and design of this study. AWH, RAM, RC, JL, ES, JJW, NGM, GWM, PM, DAM and JEC recruited participants. Genotyping was performed by KPB, PD, ACV, AKH, JJW, DRN, NGM, GWM, MAB and JEC. Statistical analysis was undertaken by KPB, SM, JZL, PL, ER, DRN and MAB. Direct sequencing was performed by KPB and AC. SS, GC, RC and JW performed the immunohistochemistry and gene expression studies. KPB, SM and JEC wrote the initial draft. All authors critically revised and provided final approval of this manuscript.

CONFLICTS OF INTEREST:

None of the authors have conflict of interest or financial interest in this work.

Figure legends

Figure 1: Association results for genotyped SNPs. SNPs with p-value reaching genome-wide significance ($p<5x10^{-8}$) are shown in black. Results are corrected for $\lambda=1.06$. Chromosome 23 refers to the X chromosome.

Figure 2: Association results for SNPs at the genome-wide significant loci, corrected for lambda of 1.06. Genotyped SNPs are indicated by solid triangles and imputed SNPs by hollow circles. The top ranked SNP at each locus is shown as a solid diamond. Imputation p-values for all SNPs are plotted. Color scheme indicates linkage disequilibrium between top ranked SNP and other SNPs in the region. Note imputed and genotyped p-values for genotyped SNPs differ slightly because for the imputed result, analysis is based on dosage scores whereas with genotyped SNPs hard genotype calls are used. A) chromosome 1q24 region. Imputation p-value was $p=1.0x10^{-9}$ for top SNP rs7524755, with the top genotyped SNP, rs4656461 the fourth best SNP after imputation, $p=1.6x10^{-9}$. B) chromosome 9p21 region. Imputation p-value was $p=3.7x10^{-9}$ for top SNP rs10757270, with top genotyped SNP, rs4977756 the second best SNP after imputation, $p=8.1x10^{-9}$.

Figure 3: Ocular expression of the genes at the glaucoma associated loci. A) Expression of the *TMCO1*, *CDKN2A*/*ARF*, *CDKN2B*, *CDKN2B-AS1* and *MTAP* genes was analyzed in various human eye tissues by RT-PCR using gene-specific primers (Supplementary Table 5). *GAPDH* was amplified to control for the amount of cDNA template used from each tissue for PCR. The expected size of each PCR product is indicated in Supplementary Table 5B) Expression of *CDKN2B-AS1* splice variants in human retina. RT-PCR was performed with gene-specific primers in exon 1 and 19 of the *CDKN2B-AS1* gene (Supplementary Table 5C). Lanes 1, 2 and 3 correspond to the splice-variants amplified upon primer annealing at 52°C, 54°C and 56°C respectively. The variant in lane 1 results from splicing of exons 1-5-6-7-19, in lane 2 from splicing of exons 1-5-6-7-10-11-13-14-15-16-17-18-19 and in lane 3 from splicing of exons 1-5-6-7-15-16-17-18-19. These variants are different to previously reported *CDKN2B-AS1* variants [11,12]. The full-length variant (DQ485453) and alternatively spliced variants (DQ485454 and GQ495924) [11,12] were undetectable in human retina (data not shown). M, molecular weight markers in basepairs; RT^-, reverse transcription negative control; -ve C, PCR negative control.

Figure 4: (**A**) Expression of *Tmco1 Cdkn2a* and *Cdkn2b* mRNAs in rat retina 7 days after induction of experimental glaucoma (mean intraocular pressure at time of death of 32±3.7 mmHg) as determined by quantitative real-time RT-PCR, where *n*=4. Error bars indicate standard error of the mean. (**B**) Axonal degeneration in the distal optic nerve of one representative animal, as evaluated by immunolabelling for non-phosphorylated neurofilament heavy protein. Numerous axonal swellings and abnormalities are visible in the optic nerve of the treated eye compared with the control optic nerve, which appears normal. Scale bar panels B-C: 25 µm.

Tables

Table 1: Demographic features of the cohorts.

	n		age			% female		
Cohort	Case	Control	Case	Control	p-value	Case	Control	p-value
Discovery	615	3956	76.6±13.9	43.4±11.5	$<1.0x10^{-6}$	52.1	78.9*	$<1.0x10^{-6}$
Advanced replication	334	434	74.9±11.7	78.7±9.1	$2.0x10^{-6}$	55.6	59.1	0.35
Less Severe replication	465	1436	71.8±12.6	52.0±0	$<1.0x10^{-6}$	61.4	49.7	$1.2x10^{-5}$
Blue Mountains Eye Study	93	2712	76.5±9.4	70.1±10.1	$<1.0x10^{-6}$	8.5	45.4	$<1.0x10^{-6}$
Combined replication	892	4582	72.0±13.0	64.9±12.4	$<1.0x10^{-6}$	51.1	47.4	0.050

* one of the two control cohorts was entirely female, discussed in main text.

Table 2: Association results for genome-wide significant genotyped SNPs in the discovery cohort and three replication cohorts. The frequency of the risk allele in cases and controls is given. All tests were performed under an allelic model.

			Discovery Cohort			Advanced glaucoma replication			Less severe glaucoma replication			Blue Mountains Eye Study		
SNP:Risk allele	Chr	Build 36 position	Frequency case/control	P-value*	OR (95% CI)	Frequency case/control	P-value	OR (95% CI)	Frequency case/control	P-value	OR (95% CI)	Frequency case/control	P-value	OR (95% CI)
rs4656461:G	1	163953829	0.19/0.12	6.1×10^{-10}	1.68 (1.43-1.98)	0.17/0.12	0.010	1.47 (1.09-1.97)	0.15/0.12	0.026	1.28 (1.03-1.59)	0.17/0.12	0.022	1.57 (1.07-2.32)
rs7518099:C	1	164003504	0.18/0.12	4.7×10^{-10}	1.67 (1.42-1.96)	0.16/0.12	0.032	1.38 (1.03-1.86)	0.15/0.12	0.022	1.29 (1.04-1.61)	0.18/0.12	0.007	1.68 (1.15-2.46)
rs4977756:A	9	22058652	0.69/0.60	4.7×10^{-09}	1.50 (1.31-1.70)	0.69/0.63	0.042	1.25 (1.01-1.56)	0.64/0.58	0.013	1.21 (1.04-1.41)	0.68/0.60	0.015	1.48 (1.08-2.04)
rs10120688:A	9	22046499	0.58/0.48	1.4×10^{-08}	1.44 (1.28-1.63)	0.56/0.52	0.153	1.16 (0.95-1.43)	0.51/0.46	0.003	1.27 (1.08-1.48)	0.57/0.48	0.025	1.40 (1.04-1.88)

* corrected for lambda of 1.06

ONLINE MATERIALS & METHODS:
Participant Recruitment:
See Supplementary Note online.

Genotyping and data quality control:
Following DNA extraction Australian twin and endometriosis sample controls were genotyped at deCODE Genetics (Reykjavik, Iceland) on Illumina HumanHap 610W Quad and Illumina Human670Quad Beadarrays, respectively. Cases were genotyped in the laboratory of MAB, on Illumina Human1M-Omni arrays. SNPs with a mean BeadStudio GenCall score <0.7 were excluded from the controls. All samples had successful genotypes for >95% of SNPs. SNPs with call rates either <0.95 (minor allele frequency, MAF > 0.05) or <0.99 (MAF > 0.01), Hardy-Weinberg equilibrium in controls $P<10^{-6}$, and/or MAF <0.01 were excluded. Cryptic relatedness was identified through the production of a full identity by state matrix and 0 cases and 72 controls were removed. Ancestry outliers were identified by principal component (PC) analysis, using data from 11 populations of the HapMap 3 and five Northern European populations genotyped by the GenomeEUtwin consortium, using the EIGENSOFT package[25] using a subset of 160,000 independent SNPs. Individuals (n=25 cases and 219 controls) lying ≥ 2 standard deviations from the mean PC1 and PC2 scores were removed[30]. Following these exclusions there were 590 cases, genotyped for 790,038 SNPs and 3,956 controls, genotyped for 518,687 SNPs. Our primary analysis was based on a common set of 298,778 SNPs. To investigate population stratification in the cleaned data set, we generated Q-Q plots. These same SNPs were used to generate the first 10 principal components for case and control samples combined using EIGENSOFT.

Genomic imputation:
Imputation for the Australian twins was performed using MACH2 with data obtained by the Centre d'Etude du Polymorphisme Humain from the 1000 Genomes reference panel 2010_03 release. Imputation was based on a set of autosomal SNPs common to all samples (n=292,883). The total number of SNPs imputed with imputation r^2>0.5 was 5,548,553 and these were taken forward for analysis.

Association analysis:
Association analysis was performed using PLINK[26]. Dosage scores from imputation analysis was performed using MACH2DAT[27]. Analysis was conducted with and without the first 10 principal components included as covariates (with negligible difference to results, data not shown). Figure 2 was prepared using LocusZoom[28].

Replication study genotyping and analysis
All genome-wide significant SNPs were further examined in an independent replication, along with additional SNPs at each locus. SNPs chosen for genotyping were those mapping to each locus defined as within annotated genes *TMCO1* (4 SNPs), *CDKN2A* (2 SNPs), *CDKN2B* (2 SNPs) or *CDKN2B-AS1* (5 SNPS) and ranked within the top 1000 genotyped SNPs. In addition, SNPs previously reported as associated with other phenotypes at the 9p21 locus but not typed in the discovery phase were also included if the assay design allowed them to multiplex with the other SNPs (4 SNPs). SNPs were genotyped using iPLEX Gold chemistry (Sequenom Inc, San Diego, CA, USA) in a single plex on an Autoflex Mass Spectrometer (Sequenom Inc.) at the Australian Genome Research Facility (Brisbane, Australia). Genotypes for controls from the BMES cohort were extracted from a previously conducted genome-wide association scan using Illumina HumanHap 670 arrays. Genotypes of the WTCCC 58BC cohort typed on the Illumina HumanHap550 array were downloaded from the European Genome-phenome Archive and the relevant SNPs extracted. Each SNP in the replication phase was checked for consistent strand and

flipped in one dataset if necessary. Association analysis was conducted in PLINK. Advanced replication cases were compared to 434 elderly examined controls. 465 less severe cases were compared to the WTCCC 58BC data (n=1436) and glaucoma cases from within the BMES (n=93) was analysed compared to all other participants with available genotype data (n=2712). Data were pooled for the combined replication cohort analyses. Age and sex were included in a logistic regression under an additive model.

Haplotype analysis:
The haplotype analysis was conducted on the combined dataset of all cases, the discovery controls and a subset of BMES controls that were genotyped in house. Analysis was conducted in PLINK. All four *TMCO1* SNPs from the replication phase were included in the haplotype. Prior to analysis, the chromosome 9 locus was assessed in this data for linkage disequilibrium structure using Haploview[29] . The "solid spine of LD" block definition was used and identified a block between SNPs rs3217992 and rs4977756, and haplotypes were calculated in this block. Inclusion of SNPs outside this block resulted in a large number of rare and less common haplotypes. Only haplotypes with frequency >1% were considered.

Resequencing:
The coding exons, 3'UTR and all splice sites of *TMCO1* were sequenced in twelve cases who were homozygous for the risk allele (G) at rs4656461. Primers are given in Supplementary Table 5. Each fragment was amplified by PCR with 0.5U of Hotstart Taq (Qiagen, Doncaster, Australia). Following clean-up of PCR products by incubation at 37^{o}C with 2U of Shrimp Alkaline Phosphatase (USB, Clevland, OH) and 10U of Exonuclease I (New England Biolabs, MA), products were directly sequenced on an ABI PRISM 3100 Genetic Analyzer (Applied Biosystems, Foster City, CA) with BigDye Terminators (Applied Biosystems) according to standard protocols.

Estimates of effect size in replication cohort
To calculate an unbiased estimate of risk for advanced glaucoma we focused on the replication cohort. Taking advanced glaucoma cases (N=334), and the full set of examined replication controls (N=936) we fitted rs4977756 and rs4656461 in a logistic regression using R[30]. Additive effects were modelled by coding SNPs as 0/1/2 risk alleles and dominance effects were modelled by coding homozygotes as 0 and heterozygotes as 1.

Expression analysis in human ocular tissue
Ocular tissues from post-mortem human eyes were obtained through the Eye Bank of South Australia, according to guidelines of the Southern Adelaide Health Service/Flinders University Human Research Ethics Committee. Total RNA was extracted using the RNeasy Mini Kit (Qiagen). First strand cDNA was synthesised using the Superscript III reverse transcriptase (Invitrogen, Australia) and random hexamers. Human retinal cDNA was synthesised using an oligo-dT primer. PCR was performed using the Hot Star Taq polymerase (Qiagen) and gene-specific primers (Supplementary Table 5B). For amplification of *CDKN2B-AS1* splice variants, PCR was performed with gene specific primer Exon 1F (forward) in combination with either Exon 19R, Exon 12-3'R or Exon 13R primer (reverse) (Supplementary Table 5C) in the presence of Q Solution (Qiagen). Specificity of each amplified products was confirmed by sequencing. Coding exons in each variant were determined from alignment with the *CDKN2B-AS1* reference sequence NR_003529.3.

Immunohistochemistry in rat ocular tissue
Tissue sections were deparaffinized in xylene and rinsed in 100% ethanol, before treatment with 0.5% H_2O_2 for 30 min to block endogenous peroxidase activity. Antigen retrieval was achieved by microwaving the sections in 10 mM citrate buffer (pH 6.0). Tissue sections were then blocked in 3% normal horse serum/ phosphate buffered saline (PBS) , incubated overnight at room temperature in primary antibody, followed by consecutive incubations with biotinylated secondary antibody

(Vector, Burlingame, CA) and streptavidin-peroxidase conjugate (Pierce, Rockford, IL). Color development was achieved with NovaRED (Vector). Sections were counterstained with hematoxylin, dehydrated and mounted. Specificity of antibody staining was confirmed by incubating adjacent sections with mouse IgG1 isotype control (BD Pharmingen) or normal rabbit serum for the monoclonal antibody and polyclonal rabbit antibodies, respectively. Primary antibodies used: anti-mouse CDKN2A (Abcam, clone 2D9A12, 1:1000), CDKN2B (Cell Signaling Technology, #4822, 1:1000), anti-rabbit TMCO1 (Aviva Systems Biology, ARP49429_P050, 1:500 to 1:1000).

For Western blotting to confirm specificity of the TMCO1 antibody, samples from rat liver, brain, retina and optic nerve were sonicated in freshly prepared 20mM Tris/HCl buffer (pH 7.4) containing 2mM EDTA, 0.5mM EGTA, the protease inhibitors phenylmethyl-sulphonyl fluoride (0.1mM), leupeptin (50 μg/ml) and aprotinin (50 μg/ml) plus a phosphatase inhibitor cocktail. An equal volume of sample buffer (62.5 mM Tris/HCl, pH 7.4, 4% SDS, 10% glycerol, 10% β-mercaptoethanol and 0.002% bromophenol blue) was added and samples were boiled for 3 min. Samples were size fractionated by SDS-PAGE and transferred onto PVDF membrane. Blot was blocked with 5% skimmed milk/Tris buffered saline containing 0.1% Tween 20, probed with antibodies to actin or TMCO1 followed by appropriate secondary antibodies conjugated to biotin, and then streptavidin-peroxidase conjugate. Blot was developed with a 0.016% solution of 3-amino-9-ethylcarbazole in 50 mM sodium acetate (pH 5) containing 0.05% Tween-20 and 0.03% H_2O_2.

Evaluation of gene expression levels in a rat model of glaucoma

Sprague-Dawley rats were anaesthetised with an intraperitoneal injection of 100 mg/kg ketamine and 10 mg/kg xylazine and local anesthetic drops applied to the eye. Ocular hypertension was induced in the right eye of each animal by laser photocoagulation of the trabecular meshwork as previously described[13]. IOPs were measured in both eyes at baseline, 8h, day 1, 3 and 7 using a rebound tonometer calibrated for use in rats. All rats were killed by transcardial perfusion with physiological saline under deep anaesthesia. The retinas were dissected for RT-PCR, while the chiasm from each rat was taken for immunohistochemistry to verify that the procedure had induced an appropriate injury response using the same method detailed above. Total RNA was isolated from each retina and first strand cDNA synthesised from 2 μg DNase-treated RNA. Duplicate real-time PCR reactions were carried out using the cDNA equivalent of 20 ng total RNA for each sample in a total volume of 25 μl containing 1 × SYBR Green PCR master mix (BioRad), in an IQ5 icycler (Bio-Rad)..Primer sets used are detailed in Supplementary Table 5. After the final cycle of the PCR, primer specificity was checked by the dissociation (melting) curve method. The relative expression in each sample was calculated using *Gapdh* as reference mRNA as previously described[31].

References

1. Quigley, H.A. & Broman, A.T. The number of people with glaucoma worldwide in 2010 and 2020. *Br J Ophthalmol* **90**, 262-7 (2006).
2. Heijl, A. et al. Reduction of intraocular pressure and glaucoma progression: results from the Early Manifest Glaucoma Trial. *Arch Ophthalmol* **120**, 1268-79 (2002).
3. Stone, E.M. et al. Identification of a gene that causes primary open angle glaucoma. *Science* **275**, 668-70 (1997).
4. Pasutto, F. et al. Heterozygous NTF4 mutations impairing neurotrophin-4 signaling in patients with primary open-angle glaucoma. *Am J Hum Genet* **85**, 447-56 (2009).
5. Rao, K.N. et al. Variations in NTF4, VAV2, and VAV3 genes are not involved with primary open-angle and primary angle-closure glaucomas in an indian population. *Invest Ophthalmol Vis Sci* **51**, 4937-41.
6. Thorleifsson, G. et al. Common variants near CAV1 and CAV2 are associated with primary open-angle glaucoma. *Nat Genet* (2010).
7. Green, C.M. et al. How significant is a family history of glaucoma? Experience from the Glaucoma Inheritance Study in Tasmania. *Clin Experiment Ophthalmol* **35**, 793-9 (2007).
8. Hewitt, A.W. et al. Sensitivity of confocal laser tomography versus optical coherence tomography in detecting advanced glaucoma. *Clin Experiment Ophthalmol* **37**, 836-41; quiz 903-4 (2009).
9. Painter, J. et al. Genome-wide association study identifies a locus at 7p15.2 associated with the development of endometriosis. *Nat Genet* **In Press**(2010).
10. Beavis, W. The power and deceit of {QTL} experiments: lessons from comparative {QTL} studies. in *Proceedings of the Corn and Sorghum Industry Research Conference* 250-266 (American Seed Trade Association, Washington D.C, 1994).
11. Folkersen, L. et al. Relationship between CAD risk genotype in the chromosome 9p21 locus and gene expression. Identification of eight new ANRIL splice variants. *PLoS One* **4**, e7677 (2009).
12. Pasmant, E. et al. Characterization of a germ-line deletion, including the entire INK4/ARF locus, in a melanoma-neural system tumor family: identification of ANRIL, an antisense noncoding RNA whose expression coclusters with ARF. *Cancer Res* **67**, 3963-9 (2007).
13. Ebneter, A., Casson, R.J., Wood, J.P. & Chidlow, G. Microglial activation in the visual pathway in experimental glaucoma: spatiotemporal characterization and correlation with axonal injury. *Invest Ophthalmol Vis Sci* **51**, 6448-60.
14. Xin, B. et al. Homozygous frameshift mutation in TMCO1 causes a syndrome with craniofacial dysmorphism, skeletal anomalies, and mental retardation. *Proc Natl Acad Sci U S A* **107**, 258-63 (2010).
15. Iwamuro, S., Saeki, M. & Kato, S. Multi-ubiquitination of a nascent membrane protein produced in a rabbit reticulocyte lysate. *J Biochem* **126**, 48-53 (1999).
16. Zhang, Z. et al. Molecular cloning, expression patterns and subcellular localization of porcine TMCO1 gene. *Mol Biol Rep* **37**, 1611-8 (2010).
17. Helgadottir, A. et al. A common variant on chromosome 9p21 affects the risk of myocardial infarction. *Science* **316**, 1491-3 (2007).
18. Scott, L.J. et al. A genome-wide association study of type 2 diabetes in Finns detects multiple susceptibility variants. *Science* **316**, 1341-5 (2007).
19. Bilguvar, K. et al. Susceptibility loci for intracranial aneurysm in European and Japanese populations. *Nat Genet* **40**, 1472-7 (2008).
20. Shete, S. et al. Genome-wide association study identifies five susceptibility loci for glioma. *Nat Genet* **41**, 899-904 (2009).
21. Jarinova, O. et al. Functional analysis of the chromosome 9p21.3 coronary artery disease risk locus. *Arterioscler Thromb Vasc Biol* **29**, 1671-7 (2009).

22. Gonzalez, S. & Serrano, M. A new mechanism of inactivation of the INK4/ARF locus. *Cell Cycle* **5**, 1382-4 (2006).
23. Williams, T.M. et al. Combined loss of INK4a and caveolin-1 synergistically enhances cell proliferation and oncogene-induced tumorigenesis: role of INK4a/CAV-1 in mammary epithelial cell hyperplasia. *J Biol Chem* **279**, 24745-56 (2004).
24. Ramdas, W.D. et al. A genome-wide association study of optic disc parameters. *PLoS Genet* **6**, e1000978.
25. Price, A.L. et al. Principal components analysis corrects for stratification in genome-wide association studies. *Nat Genet* **38**, 904-9 (2006).
26. Purcell, S. et al. PLINK: a tool set for whole-genome association and population-based linkage analyses. *Am J Hum Genet* **81**, 559-75 (2007).
27. Li, Y., Willer, C., Sanna, S. & Abecasis, G. Genotype imputation. *Annu Rev Genomics Hum Genet* **10**, 387-406 (2009).
28. Pruim, R. et al. LocusZoom: Regional visualization of genome-wide association scan results. . *Bioinformatics* **(In Press)**(2010).
29. Barrett, J.C., Fry, B., Maller, J. & Daly, M.J. Haploview: analysis and visualization of LD and haplotype maps. *Bioinformatics* **21**, 263-5 (2005).
30. R Development Core Team. R: A language and environment for statistical computing. *R Foundation for Statistical Computing* **2008**.
31. Pfaffl, M.W. A new mathematical model for relative quantification in real-time RT-PCR. *Nucleic Acids Res* **29**, e45 (2001).

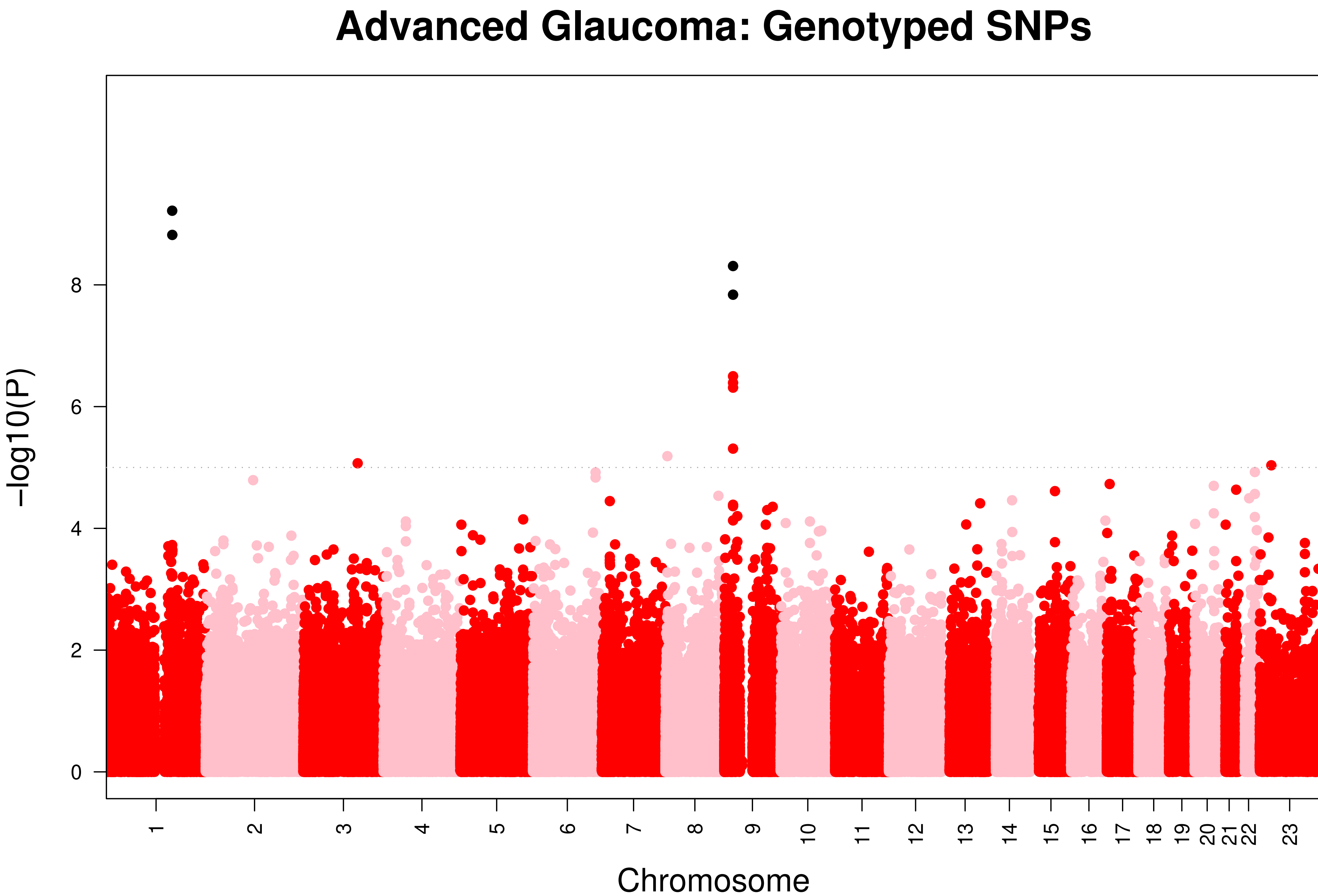

Advanced Glaucoma: Genotyped SNPs
−log10(P)
0
2
4
6
8
Chromosome
1
2
3
4
5
6
7
8
9
10
11
12
13
14
15
16
17
18
19
20
21
22
23

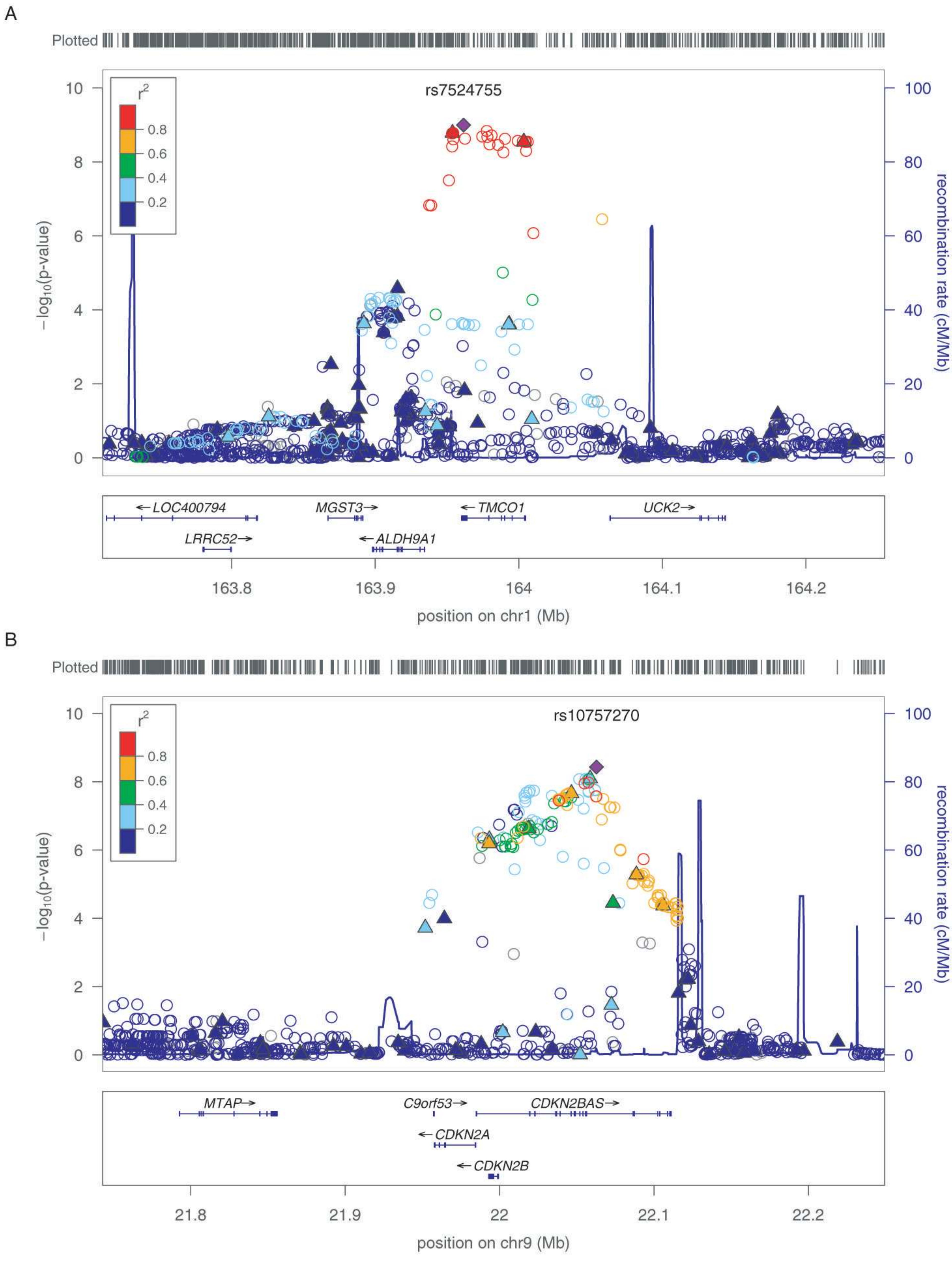

A
Plotted
rs7524755
r2
0.8
0.6
0.4
0.2
−log10(p-value)
recombination rate (cM/Mb)
LOC400794
MGST3
TMCO1
UCK2
LRRC52
ALDH9A1
163.8
163.9
164
164.1
164.2
position on chr1 (Mb)
B
Plotted
rs10757270
MTAP
C9orf53
CDKN2BAS
CDKN2A
CDKN2B
21.8
21.9
22
22.1
22.2
position on chr9 (Mb)

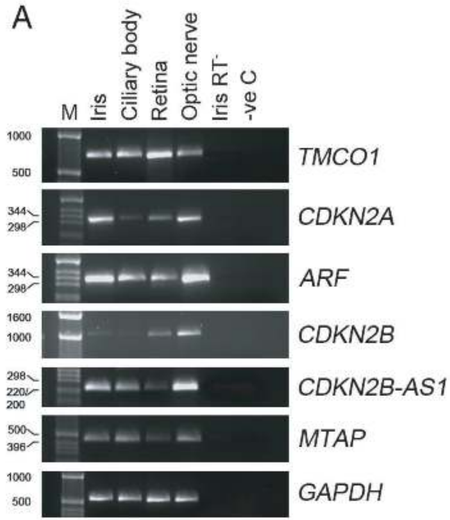
A
M
Iris
Ciliary body
Retina
Optic nerve
Iris RT-
-ve C
1000
500
TMCO1
344
298
CDKN2A
344
298
ARF
1600
1000
CDKN2B
298
220
200
CDKN2B-AS1
500
396
MTAP
1000
500
GAPDH
B
RT
M
1
2
3
-ve C
2000
1600
1000
500

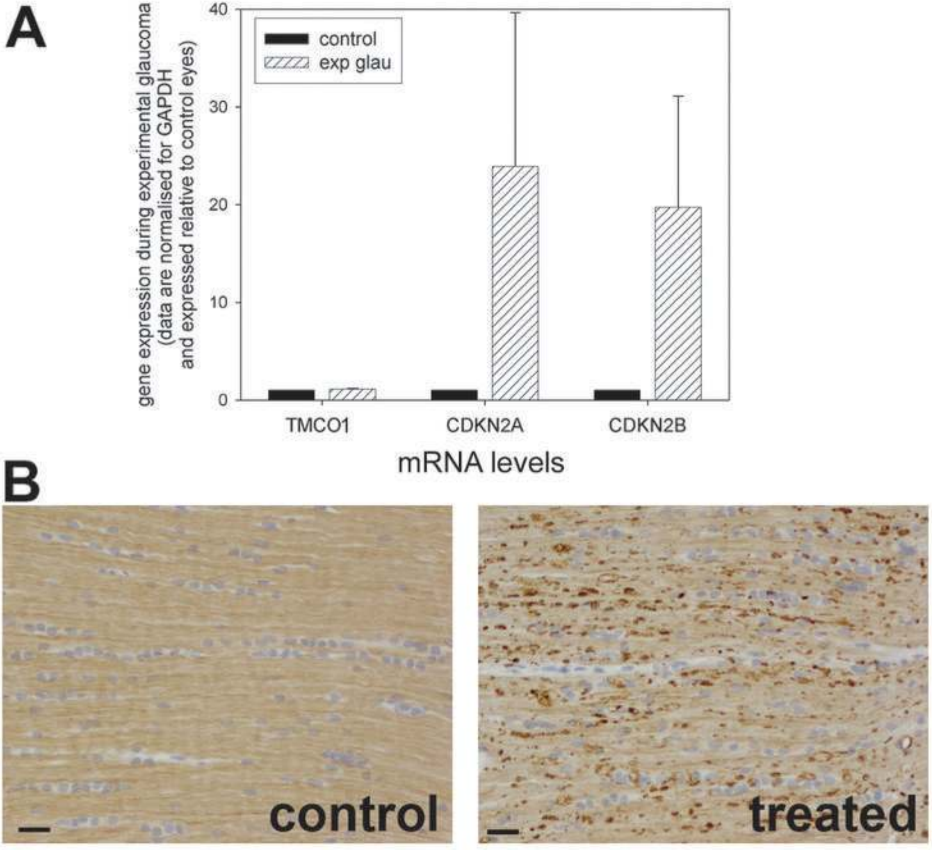
A
gene expression during experimental glaucoma
(data are normalised for GAPDH
and expressed relative to control eyes)
control
exp glau
0
10
20
30
40
TMCO1
CDKN2A
CDKN2B
mRNA levels
B
control
treated